a) 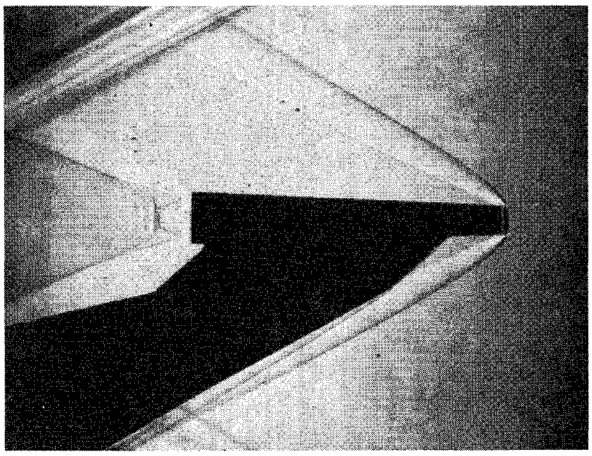

b) 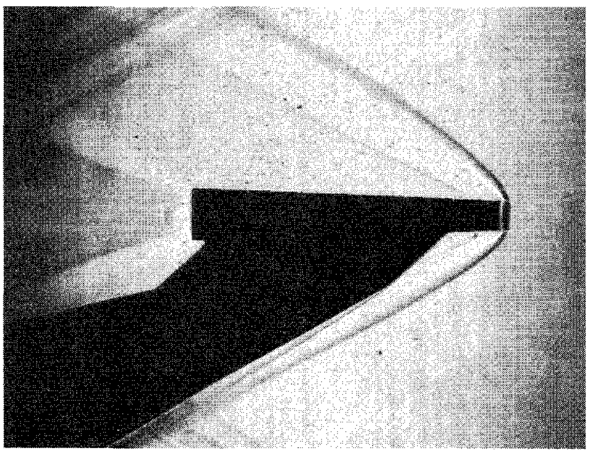

Fig. 3 a) Configuration 3, smooth through-flow channel with tube restriction, $\alpha = 0$ deg and b) configuration 4, through-flow restricted by a tube and screen, $\alpha = 0$ deg.

The exit flow in the first case, configuration 3, with only the tube restriction, is most certainly supersonic due to the converging–diverging nozzle effect of the restriction (Fig. 1b), about Mach 1.8. The exit flow in Fig. 3a shows the multiple shocks required to slow the internal flow down to freestream conditions. Assuming supersonic internal flow, a capture area ratio of 0.73 and mass flow rate of 0.0099 kg/s can be calculated.

Figure 3b shows the second case, configuration 4, with a screen added upstream of the tube. Here, evidently the flow lost enough stagnation pressure through the screen so that the flow within the nacelle and at the exit stays subsonic.

Conclusions

A supersonic engine nacelle with a flow-through channel was tested at a Mach number of 1.94 at a model length Reynolds number of 2.5×10^6: with a smooth constant diameter flow-through channel, with a rough constant diameter flow-through channel, and two cases where the channel was restricted. The test conclusions are as follows:

1) In the smooth constant diameter channel case the flow was unchoked and the bow shock was attached.

2) With a rough constant diameter channel, the flow was choked, resulting in a detached bow shock, but an exit flow structure similar to the unchoked case.

3) The two cases where the flow channel was restricted, first with a tube and second with the tube and a screen, the bow shock was detached and the exit flow was unlike case 1 or 2.

4) It can be concluded that for a particular model geometry, freestream Mach number, and pressure the exit flow structure of an adiabatic flow-through channel is only dependent on the exit flow Mach number.

References

[1]Irani, E., and Ellis, D. R., "Supersonic Wind-Tunnel Visualization of Shock Structures on Flow Through Engine Nacelles," National Institute for Aviation Research, Rept. 92-16, Wichita, KS, Sept. 1992.

[2]Goldstein, R. J., "Optical Systems for Flow Measurement: Shadowgraph, Schlieren, and Interferometric Techniques," *Fluid Mechanics Measurements*, Hemisphere, Washington, DC, 1983, pp. 377–422.

[3]Pope, A., and Goin, K. L., "Calibration and Use of Supersonic Tunnels," *High Speed Wind Tunnel Testing*, Wiley, New York, 1965, pp. 383, 384.

[4]Shapiro, A. H., "Flow in Constant-Area Ducts with Friction," *The Dynamics and Thermodynamics of Compressible Fluid Flow*, Wiley, New York, 1953, pp. 162–173.

[5]Anderson, J. D., Jr., *Modern Compressible Flow with Historical Perspective*, McGraw–Hill, New York, 1990, pp. 85–91.

Origin of Computed Unsteadiness in the Shear Layer of Delta Wings

Miguel R. Visbal* and Raymond E. Gordnier*
U.S. Air Force Wright Laboratory,
Wright–Patterson Air Force Base, OH 45433-7913

Introduction

EXPERIMENTAL observations[1-4] of the shear layer emanating from the leading edge of delta wings have revealed the existence of both steady and unsteady vortical substructures somewhat reminiscent of the classical Kelvin–Helmholtz instability found in plane shear layers. Previous computations by the present authors[5] for a 75-deg sweep delta wing at low Reynolds number also showed the presence of unsteady, three-dimensional, vortical structures in the shear layer. Frequencies were commensurate with experiments[1,2] as well as with those obtained from an inviscid linear two-dimensional stability analysis.

Recently, it has been suggested[3,4] that the unsteady type of shear-layer instability on delta wings (with which this Note is solely concerned) is simply caused in the experiments by flow disturbances inherent to the experimental setup. Given the sensitivity of shear layers to natural disturbances, this is a reasonable explanation in the experimental situation where environmental and surface disturbances are present. However, it raises the question as to the origin of the unsteadiness observed in the computations in which no deliberate forcing of the shear layer is applied. If one assumes the spatially developing, three-dimensional shear layer above the delta wing to be convectively unstable, a continuous forcing is required for the shear-layer roll-up process to persist. The purpose of this Note is to elucidate the origin of the computed unsteadiness previously reported.[5]

Results and Discussion

In the interpretation of the computed and experimental work cited earlier, emphasis has been placed almost exclu-

Received Aug. 4, 1994; revision received Feb. 14, 1995; accepted for publication Feb. 24, 1995.

*Aerospace Engineer, CFD Research Branch, Aeromechanics Division. Senior Member AIAA.

sively on the vortex sheet emanating from the leading edge and on the possible instabilities to which it may be susceptible. An additional aspect of the flow that has not been considered is the interaction of the leading-edge primary vortex with the surface. It is well-known that regions of concentrated vorticity in proximity to a solid surface can promote, due to the induced adverse pressure gradient, an eruptive response or unsteady separation in the boundary layer. Several examples of this phenomenon are discussed in the recent review by Doligalski et al.[6]

As shown below, the process of boundary-layer eruption induced by the interaction of the primary vortex with the wing upper surface is strongly linked to the shear-layer unsteadiness found computationally in Ref. 5. To illustrate this point, computations are performed for delta wings at an angle of attack $\alpha = 20.5$ deg and a freestream Mach number $M_\infty = 0.2$. Two different wing sweep angles ($\Lambda = 75$ and 85 deg) and chord Reynolds numbers ($Re_C = 10^4, 5 \times 10^4$) are considered. This configuration and these flow conditions include the case previously studied in Ref. 5. The flowfields are simulated by solving the three-dimensional, unsteady full Navier–Stokes equations employing the implicit Beam–Warming algorithm. Reference 5 provides further details, including the grid structure and boundary conditions.

Figure 1a shows contours of the X component of vorticity on a crossflow plane ($X/C = 0.7$) at a given instant during the unsteady process of the baseline case ($\Lambda = 75$ deg, $Re_C = 5 \times 10^4$). The roll-up of the shear layer above the wing is clearly visible and a complete description of this process is given in Ref. 5. Another feature apparent in Fig. 1a is the secondary separation of the boundary layer developing along the wing surface and the resulting upward ejection of vorticity. The importance of this effect in regard to the overall unsteady process is examined next.

To explore the influence of unsteady, secondary separation on the shear layer, wall suction is applied on the wing upper surface. A constant suction velocity $W_s = 0.05U_\infty$ is prescribed over the area bounded by $0.05 \leq X/C \leq 0.97$ and $0.48 \leq Y/S \leq 0.98$, where S denotes the local wing semispan. This suction magnitude and extent are not intended to represent a realistic control situation, but are used simply to investigate the origin of flow unsteadiness. After suction is applied, a fully converged steady flowfield is achieved, as shown in Fig. 1b, and the shear-layer substructures are absent. Clearly, the prevention of unsteady secondary boundary-layer separation also results in the elimination of the shear-layer roll-up or instability. When the suction is turned off, the unsteady shear-layer phenomenon returns. The present results strongly suggest that the shear-layer instability found computationally[5] is driven by a boundary-layer eruptive process induced by the vortex/surface interaction. Recent instantaneous high-resolution velocity measurements[7] confirm the numerically predicted strong vortex/surface interaction and wall vorticity ejection.

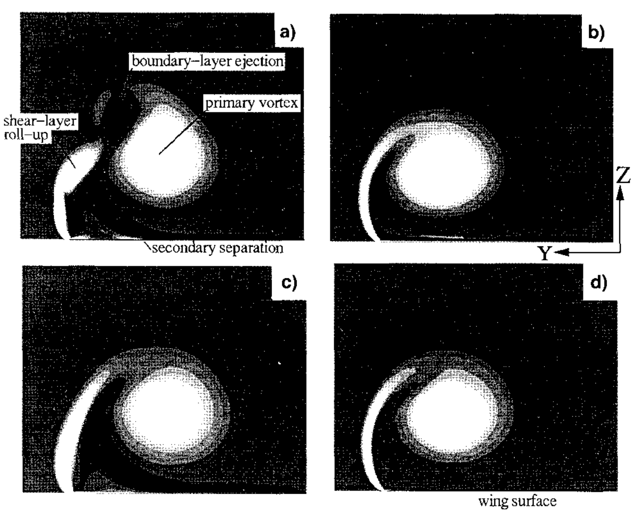

Fig. 1 X component of vorticity on crossflow plane $X/C = 0.7$ for $\Lambda = 75$ deg. White and black contours correspond to positive and negative vorticity, respectively: a) baseline case, $Re_C = 5 \times 10^4$; b) suction applied on wing upper surface, $Re_C = 5 \times 10^4$; c) $Re_C = 10^4$; and d) Euler solution.

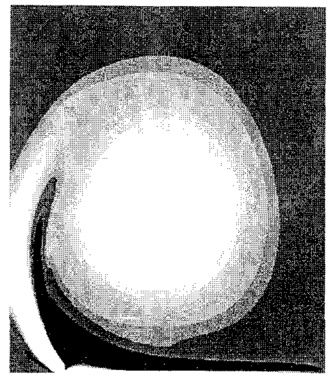

Fig. 2 X component of vorticity on crossflow plane $X/C = 0.7$ for $\Lambda = 85$ deg and $Re_C = 5 \times 10^4$.

As discussed in Ref. 6, the eruptive response of the near-wall flow in a vortex/surface interaction depends in general on the Reynolds number as well as on the strength and position of the vortex above the surface. Therefore, it is expected that in the delta wing configuration increasing the Reynolds number or angle of attack, or reducing leading-edge sweep promotes unsteady boundary-layer separation and shear-layer roll-up. To investigate the effect of Reynolds number, the previous flowfield is recomputed for a lower Reynolds number ($Re_C = 10^4$). The result, shown in Fig. 1c, displays no shear-layer unsteadiness in agreement with the experiment of Reynolds and Abtahi.[3] This seems to indicate that below certain value of Re_C (which depends on angle of attack and wing sweep), the boundary-layer ejection process is not present, and as a result the shear-layer instability is not excited (in the absence of other perturbations).

Since increasing the wing leading-edge sweep reduces the strength of the primary vortex, it is also expected that the effect of higher Λ is to inhibit unsteady, boundary-layer separation and shear-layer instability. To demonstrate the effect of sweep angle, the case of $\Lambda = 85$ deg and $Re_C = 5 \times 10^4$ is computed. As shown in Fig. 2, boundary-layer ejection and roll-up of the shear layer are not present for the higher sweep. Although not included here, the flowfield for $\Lambda = 85$ deg and $\alpha = 20.5$ deg is found to remain steady for a Reynolds number as high as 4×10^5. On the other hand, reducing the wing sweep angle should enhance the vortex/surface interaction and may explain the unsteadiness observed by Gad-el-Hak and Blackwelder[1] at low Reynolds numbers for $\Lambda = 45$ and 60 deg.

Since inviscid solutions for sharp-edge delta wings are commonly used, it is of interest to examine the shear-layer behavior for Euler computations. The result for $\Lambda = 75$ deg obtained by solving the Euler equations is shown in Fig. 1d. In this case, no unsteady shear-layer substructures are observed, and the solution converges to a steady state. Although this computed inviscid flow cannot be compared directly with the actual viscous situation, it reinforces the fact that without secondary separation no shear-layer instabilities are found computationally.

Summary

This Note investigates the origin of the computed instability in the shear layer of delta wings for low Reynolds number, laminar conditions. The present results demonstrate that the computed shear-layer unsteadiness and roll-up are closely linked to the boundary-layer eruptive behavior induced by the vortex/surface interaction. Increasing Reynolds number and lowering leading-edge sweep are found to enhance this effect. Although the main objective is to provide an explanation of the computed shear-layer unsteady process, it is clear that the described eruptive near-wall phenomenon is important in the interpretation of experimental results as well. Finally, one must recognize that shear-layer unsteadiness could also be promoted by other mechanisms such as freestream disturbances and the onset of vortex breakdown at higher angles of attack.

References

[1]Gad-el-Hak, M., and Blackwelder, R. F., "The Discrete Vortices from a Delta Wing," *AIAA Journal*, Vol. 23, No. 6, 1985, pp. 961, 962.

[2]Lowson, M. V., "The Three-Dimensional Vortex Sheet Structure on Delta Wings," *Fluid Dynamics of Three-Dimensional Turbulent Shear Flows and Transition* (Cesme, Turkey), Oct. 1988, pp. 11-1–11-16 (AGARD-CP-438).

[3]Reynolds, G., and Abtahi, A., "Three-Dimensional Vortex Development, Breakdown and Control," AIAA Paper 89-0998, March 1989.

[4]Washburn, A. E., and Visser, K. D., "Evolution of Vortical Structures in the Shear Layer of Delta Wings," AIAA Paper 94-2317, June 1994.

[5]Gordnier, R. E., and Visbal, M. R., "Unsteady Vortex Structure over a Delta Wing," *Journal of Aircraft*, Vol. 31, No. 1, 1994, pp. 243–248.

[6]Doligalski, T. L., Smith, C. R., and Walker, J. D. A., "Vortex Interactions with Walls," *Annual Review of Fluid Mechanics*, Vol. 26, 1994, pp. 573–616.

[7]Ding, Z., Shih, C., and Lourenco, L., "Leading Edge Vortices of a Delta Wing Flow Field," AIAA Paper 95-0652, Jan. 1995.

Oscillatory Behavior of Helicopter Rotor Airloads in the Blade Stall Regime

K. V. Truong* and J. J. Costes†
ONERA, BP 72-92322 Châtillon, France

Introduction

IT is now well established[1] that the retreating blade stall regime of a helicopter rotor is dominated by dynamic vortex-shedding phenomena. Based on laser velocimeter measurements, Young and Hoad[2] found that a series of vortices are shed at regular time intervals from a stalled airfoil at Mach number $M = 0.49$, but inconclusive results were obtained at lower Mach $M = 0.15$. However, recent experimental investigations of the flowfield of an oscillating airfoil[3] show evidence of the occurrence of multiple vortices at relatively low Mach, i.e., at $M = 0.019$. A modeling study, based on the assumption that multiple vortices are shed periodically from the leading edge of an airfoil, shows undulatory behavior of unsteady airloads of a stalled airfoil.[4,5] One can expect that multiple vortices are released during the blade stall regime of a helicopter rotor and this phenomenon would induce an oscillatory time-varying behavior of rotor airloads, as for a stalled airfoil. In this short Note, we propose to show the existence of oscillations on airloads of a stalled rotor blade, by using a research rotor code that integrates the dynamic stall model established in Refs. 4 and 5 and by corroborating the calculated results with experimental results on a rotor in a wind tunnel.

Received June 17, 1994; revision received March 1, 1995; accepted for publication March 1, 1995.

*Research Engineer.
†Senior Scientist.

Modeling Approach

The examined experimental results were obtained in the S1 Modane wind tunnel on an articulated four-bladed rotor. The blades were instrumented with 100 pressure transducers at 5 spanwise locations, 20 hot films gauges, and 30 strain gauges. The blade deformation was measured by using the strain-pattern-analysis technique.[6]

In the research aeroelastic code used, the following assumptions are made: 1) the blade movement (which includes its forced motion and its deformation), is taken from measurements; 2) the induced flow is described by the Meijer–Drees theory[7]; and 3) the drag coefficient is supposed constant for simplification and the lift coefficient is based on the dynamic stall model established in Ref. 4.

Let us summarize the theoretical assumptions of this dynamic stall model used. It is based on the consideration of two fluid-flow mechanisms: 1) stall delay and 2) vortex-shedding phenomena. Above a critical value of the angle of attack, flow separates and vortices are shed from the airfoil. Stall delay phenomena determine the value of the angle of attack for flow separation. Stall onset is identified as a Hopf bifurcation, i.e., the replacement of steady equilibrium state of the flow by a periodic equilibrium state. According to this mathematical model, vortices are shed at regular time intervals with a characteristic frequency called Strouhal frequency, by analogy with flow past a cylinder. Beyond the Hopf bifurcation, the lift coefficient C_L has a steady component C_{L_s} and an unsteady component C_{L_u}:

$$C_L = C_{L_s} + C_{L_u} \tag{1}$$

The steady component C_{L_s} is governed by a first-order ordinary differential equation (ODE):

$$\frac{dC_{L_s}}{dt} + bC_{L_s} = bC_{L_s}^{\text{equil}}[\alpha(t), q(t)] + g_1\dot{\alpha}(t) + g_2\ddot{\alpha}(t) + g_3\dot{q}(t) + g_4\ddot{q}(t) + \vartheta(\dddot{\alpha}, \dddot{q}) \tag{2}$$

where α is the angle of attack, q the pitch rate, $C_{L_s}^{\text{equil}}$ the static value of the lift coefficient; b, g_1, g_2, g_3, and g_4 are constants and $\vartheta(\dddot{\alpha}, \dddot{q})$ designates all the $\dddot{\alpha}$ and $\dddot{q}$ terms that are negligible. The derivation of Eq. (2) is done in Ref. 4. The values of the five constants b, g_1, g_2, g_3, and g_4 can be derived from two-dimensional unsteady experiments in the regime of attached flow. The unsteady flow has two different regimes, depending upon the history of $\alpha(\xi)$ (ξ: time, varying from the origin of time to the time of observation t). When $\alpha(\xi)$ increases from zero and exceeds a critical value α_{cr}^+ (which can be significantly greater than α_{cr}, the static critical value of the angle of attack), periodic time-varying equilibrium flow replaces the steady time-invariant equilibrium. When α decreases after exceeding α_{cr}^+, the flow reattaches to the airfoil at a critical value α_{cr}^- (which can be significantly lower than α_{cr}), in these conditions, the periodic time-varying equilibrium state decays to zero. It is shown in Ref. 4 that C_{L_u} obeys a Van-der-Pol–Duffing type equation during the establishment of the periodic time-varying regime of the flow:

$$\ddot{C}_{L_u} - \omega_S(\beta_L^+ - \gamma_L^+ C_{L_u}^2)\dot{C}_{L_u} + \omega_S^2(C_{L_u} - \eta_L^+ C_{L_u}^3) = -E_L^+\omega_S\dot{\alpha} - D_L^+\ddot{\alpha} \tag{3}$$